Weighing Polyelectrolytes Packaged in Viruslike Particles

Guillaume Tresset,* Mouna Tatou, Clémence Le Cœur,† Mehdi Zeghal, Virginie Bailleux, and Amélie Lecchi
Laboratoire de Physique des Solides, Université Paris-Sud, CNRS, 91400 Orsay, France

Katarzyna Brach and Magdalena Klekotko
Institute of Physical and Theoretical Chemistry, Wrocław University of Technology, 27 Wybrzeże Wyspiańskiego, 50-370 Wrocław, Poland

Lionel Porcar
Institut Laue Langevin, 6 rue Jules Horowitz, 38042 Grenoble Cedex 9, France
(Received 7 April 2014; published 19 September 2014)

This Letter reports on the remarkable selectivity of capsid proteins for packaging synthetic polyelectrolytes in viruslike particles. By applying the contrast variation method in small-angle neutron scattering, we accurately estimated the mean mass of packaged polyelectrolytes $\langle M_p \rangle$ and that of the surrounding capsid $\langle M_{\mathrm{cap}} \rangle$. Remarkably, the mass ratio $\langle M_p \rangle / \langle M_{\mathrm{cap}} \rangle$ was invariant for polyelectrolyte molecular weights spanning more than 2 orders of magnitude. To do so, capsids either packaged several chains simultaneously or selectively retained the shortest chains that could fit the capsid interior. Our data are in qualitative agreement with theoretical predictions based on free energy minimization and emphasize the importance of protein self-energy. These findings may give new insights into the nonspecific origin of genome selectivity for a number of viral systems.

DOI: 10.1103/PhysRevLett.113.128305 PACS numbers: 82.35.Rs, 61.05.fg, 64.75.Yz, 87.14.E-

Many viruses are made up of a protein capsid protecting the genome encoded in one or more polynucleotide chains. Genome packaging can be a highly selective albeit elusive self-assembly process. For instance, cowpea chlorotic mottle virus (CCMV)—a nonenveloped icosahedral single-stranded RNA (ssRNA) plant virus—has a multipartite genome consisting of four ssRNA segments distributed in three indistinguishable particles: RNA 1 and 2 are packaged separately and have 3171 and 2774 nucleotides, while RNA 3 and 4 are packaged together and have 2173 and 824 nucleotides. In other words, all particles package more or less the same mass of RNA. Such a level of selectivity is often ascribed to intricate molecular recognitions. However, for the simplest icosahedral viruses, the packaging problem can be regarded as charged chains interacting with a rigid shell through nonspecific electrostatic interactions [1–3]. One of the most intriguing results was obtained by Belyi and Muthukumar who reported an experimental ratio of ~ -1.6 between the total charge of the genome and the net charge on the capsid interior for a wide range of simple ssRNA viruses [4]. Furthermore, theoretical predictions based on free energy minimization indicated a linear relationship between the total number of packaged monomers and the capsid interior area [2,5].

Flexible negatively charged homopolymers are excellent models to assess the selective capabilities of capsid proteins —also called capsomers—in the absence of specific molecular recognition. Poly(styrene sulfonic acid) (PSS) mimics the linear charge density ($\sim 0.33\ e^- \cdot \text{Å}^{-1}$) and the intrinsic persistence length (~ 1 nm) of ssRNA. Owing to its hydrophobic backbone, however, its intrinsic excluded volume is smaller than that of ssRNA, and ssRNA has a branched topology due to base pairing. Viruslike particles (VLPs) derived from CCMV can self-assemble with PSS, whose molecular weight determines the size of VLPs with discretized values [6,7]. The packaging process is reminiscent of the coil-globule transition of PSS in the presence of oppositely charged agents [8]. Cadena-Nava and coworkers proposed a fluorescence assay to estimate the number of packaged PSS chains per VLP [9]. However, the number of capsids was inferred from gel electrophoresis, which can be inaccurate, and the work was limited to a single PSS molecular weight. VLPs derived from the Hibiscus chlorotic ringspot virus were reported to package an amount of PSS comparable to the weight of the native genome [10], but the packaging efficiencies were estimated by destructive bulk assays which lacked reliability. To date, no systematic and accurate experimental investigation has been carried out to establish a relationship between the amounts of packaged polyelectrolytes and capsomers. Apart from its biological relevance, such a knowledge may support the development of functional VLPs for use in nanotechnology and medicine [11].

We applied the contrast variation method in small-angle neutron scattering (SANS) on a wide range of deuterated PSS (dPSS) packaged in CCMV VLPs. This nondestructive method allowed the estimation of both the mass of packaged dPSS and that of the surrounding capsid. Data were collected on the D22 beam line at the Institut Laue Langevin, a neutron source delivering one of the highest

TABLE I. Mass distribution of dPSS chains. The values were calculated from data supplied by the manufacturer and from an estimated degree of sulfonation of $95 \pm 3\%$.

dPSS	M_w [a] (kDa)	M_n [b] (kDa)	σ_n [c] (kDa)	N_n [d]
8 k	7.824	7.535	1.702	40
120 k	124.7	117.5	32.68	625
600 k	619.8	590.9	148.4	3143
1500 k	1662	1445	603	7686

[a]Weight-average mass.
[b]Number-average mass.
[c]Mass standard deviation.
[d]Number-average degree of polymerization.

fluxes worldwide. The particles were highly concentrated especially in order to detect packaged polyelectrolytes which were in minute amounts. A detailed description of sample preparations and measurements is given in the Supplemental Material [12], and the characteristics of the dPSS chains used in this study are summarized in Table I.

Upon mixing dimeric capsomers and viral RNA at a mass ratio of 6:1 in neutral buffer [12], then after dialyzing in acidic buffer, all viral RNA was spontaneously packaged in VLPs and no empty capsids were formed as demonstrated by Cadena-Nava and co-workers [21]. VLPs were afterwards concentrated up to a protein concentration of 4–5 mg/mL. The concentration of VLPs was postassembly so that mass action was not altered at the relatively high concentrations at which the scattering measurements were done. Figure 1 shows SANS patterns collected after dialysis of the samples against acidic buffer prepared with two different D_2O fractions. A fitted shell model (see Fig. 1, inset) gave a good agreement with the data in 68% D_2O and allowed the computation of the capsid volume, and, subsequently, of its mass. The latter was thus estimated to be 3.66 ± 0.345 MDa while that of the native virion is known to be 3.66 MDa, which confirmed that VLPs packaging viral RNA were morphologically identical to native virions. The right panel of Fig. 1 shows the patterns of packaged viral RNA. The region of very small wave numbers q was fitted with the Guinier approximation, i.e., $I(q) \approx I_0 \exp(-R_g^2 q^2/3)$, where R_g is the radius of gyration, valid only for $qR_g \lesssim 1$, and we thus obtained a reliable extrapolation of I_0 which can be generally expressed by

$$I_0 = K(\bar{v}, \Delta\bar{\rho}) c \langle M^2 \rangle, \quad (1)$$

where $K(\bar{v}, \Delta\bar{\rho})$ is a constant depending upon the specific volume $\bar{v}$ and the scattering length density contrast $\Delta\bar{\rho}$, c is the molar concentration, and $\langle M^2 \rangle$ is the mean squared mass. $\Delta\bar{\rho} \equiv \bar{\rho} - \rho_S$, where $\bar{\rho}$ denotes the scattering length density of the scatterers and ρ_S is that of the solvent. K can be computed from $K = (\bar{v}\Delta\bar{\rho})^2/N_A$ with N_A being Avogadro's number. Given that VLPs packaging viral RNA were reasonably monodisperse, we set

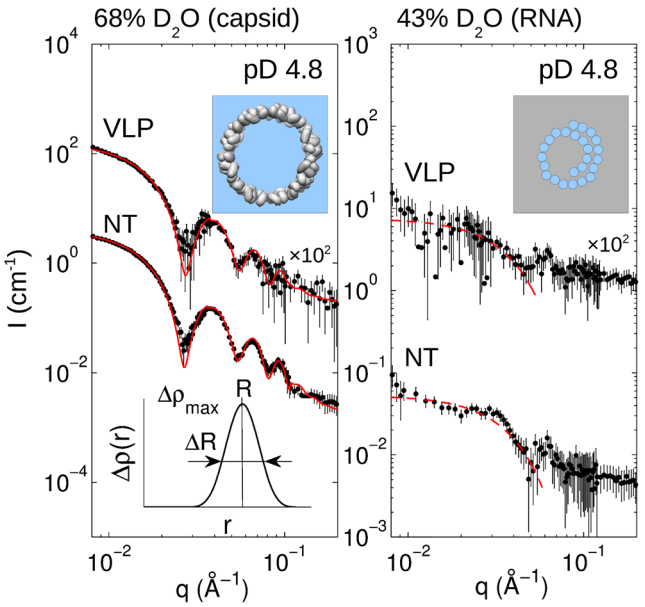

FIG. 1 (color online). SANS patterns of native (NT) virions and VLPs packaging viral RNA (VLP) at pD 4.8. (Left) In 68% D_2O, viral RNA is contrast matched and the scattering intensity I solely arises from capsomers (gray in top inset). Experimental data (black dots) are fitted with a shell model (red solid lines) defined by a scattering length density contrast $\Delta\rho(r)$ following a spline function (bottom inset): R is the mean radius, ΔR the half width of the spline, and $\Delta\rho_{\max}$ the maximal scattering length density contrast. (Right) In 43% D_2O, the contrast of capsomers vanishes and only viral RNA (blue in inset) contributes to I. A Guinier fit (red dashed lines) is plotted on each experimental curve (black dots) for small q values. The patterns are shifted for clarity.

$\langle M_{\mathrm{RNA}}^2 \rangle \approx \langle M_{\mathrm{RNA}} \rangle^2$. The mass of packaged viral RNA was determined through Eq. (1) by computing the ratio of I_0 at 43% D_2O and at 68% D_2O, and by using the capsid mass estimated from the shell model [12]. We found a mass of packaged viral RNA of 938 ± 149 kDa, that is, very consistent with our measured and expected value of ~960 kDa for native virions.

Figures 2(a) and 2(b) depict SANS patterns obtained with VLPs packaging dPSS at pD 7.5 and 4.8, respectively. Dimeric capsomers and dPSS were mixed in neutral buffer at a mass ratio of 6:1 and VLPs were concentrated up to a final protein concentration of 4–5 mg/mL. For samples at pD 4.8, the mixture was dialyzed against acidic buffer prior to concentration. The samples were then dialyzed against the same buffer containing various D_2O fractions. The residual free dimeric capsomers had a negligible contribution to the scattering intensities due to their low molecular weight. We employed a polydisperse shell model to account for the variability exhibited by these particles morphologically less regular than those packaging viral RNA. Observations by cryotransmission electron microscopy on VLPs packaging dPSS-1500k at pD 4.8 revealed a bimodal size distribution [12]. The presence of "large" VLPs—possibly along with empty capsids—was

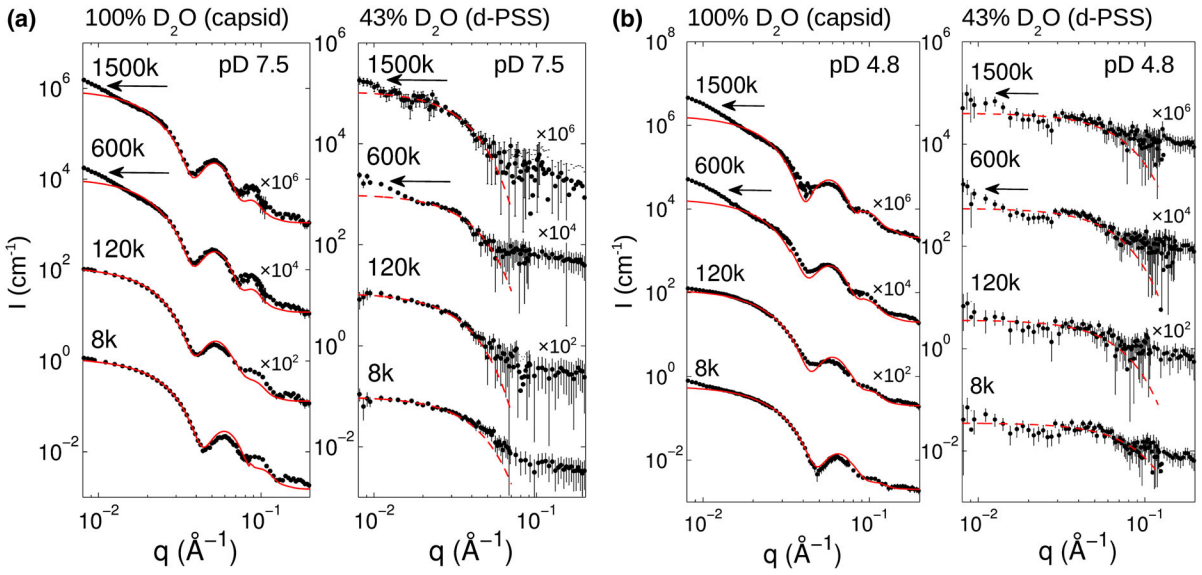

FIG. 2 (color online). SANS patterns of VLPs packaging dPSS at pD 7.5 (a) and pD 4.8 (b). (Left panels) In 100% D_2O, I is only due to capsomers. Experimental data (black dots) for various dPSS (see Table I) are fitted with a polydisperse shell model (red solid lines) based on that described in Fig. 1 except that R follows a normal distribution. (Right panels) In 43% D_2O, the patterns arise from dPSS only. A Guinier fit (red dashed line) is plotted on each experimental curve (black dots) for small q values. In all panels, the arrows indicate the contribution from large VLPs. The patterns are shifted for clarity.

evidenced on the SANS patterns by an increase of intensity at very small q values only for samples with dPSS-600k and dPSS-1500k (see arrows in Fig. 2). Such a coexistence of "small" and large VLPs was reported before [6], and theory indicates that the formation of small VLPs is entropically more favorable than large ones [22]. In this study, we only focused on small VLPs. The maximal shell diameters varied from 21.6 to 24.8 nm at pD 7.5 depending on dPSS, whereas it was 29.2 nm for native virion [12]. At pD 4.8, VLPs were smaller and the polydisperse shell model returned maximal diameters between 20.6 and 21.6 nm. The half-width of the shells varied around 4 nm for VLPs packaging dPSS whereas it was about 3 nm for native virions and VLPs packaging viral RNA. The polydispersity on the mean radius was between 5% and 10% with dPSS. These data suggest that in the presence of dPSS, capsomers were slightly disordered within the capsids. Viral RNA may therefore play a structural role that cannot be fulfilled by dPSS.

The mean squared mass of packaged dPSS $\langle M_p^2 \rangle$ was inferred from the ratio of I_0 at 100% D_2O and at 43% D_2O, and by using the mean mass of capsids $\langle M_{\rm cap} \rangle$ obtained from the polydisperse shell model. However, the significant polydispersity of dPSS chains prohibited the approximation $\langle M_p^2 \rangle \approx \langle M_p \rangle^2$, and we had to devise a statistical model estimating reliably $\langle M_p \rangle$. Accordingly, we identified two regimes depending on $\langle M_p^2 \rangle$ and the mean squared mass of free dPSS $\langle M_f^2 \rangle = M_n^2 + \sigma_n^2$. (i) If $\langle M_p^2 \rangle > \langle M_f^2 \rangle$, more than one chain is packaged on average in each VLP. Assuming that each chain has an equal probability to be packaged, the number of packaged chains per VLP is governed by the classical Poisson statistics. Since the packaged chains follow a mass distribution $n(M)$ with mean value M_n and standard deviation σ_n, $\langle M_p \rangle$ is expressed by

$$\langle M_p \rangle = \sum_{k=0}^{+\infty} \frac{\lambda^k}{k!} e^{-\lambda} \int_{-\infty}^{+\infty} n(M_1) \ldots n(M_{k+1}) dM_1 \ldots dM_{k+1} \times \sum_{j=1}^{k+1} M_j = (\lambda + 1) M_n = \langle N_p \rangle M_n, \quad (2)$$

where λ denotes the parameter of the Poisson distribution and $\langle N_p \rangle$ the mean number of packaged chains. We rule out the possibility of having empty capsids because they cannot be formed at pD 7.5 and if any at pD 4.8, their patterns will be indistinguishable from those of large VLPs. $\langle M_p^2 \rangle$ is computed similarly and gives a less trivial relationship involving λ which is substituted by its expression in Eq. (2). After some algebra, it reduces to

$$\langle M_p \rangle = \frac{1}{2} \left\{ \left[\left(1 + \frac{\sigma_n^2}{M_n^2} \right)^2 + 4 \left(1 + \frac{\langle M_p^2 \rangle}{M_n^2} \right) \right]^{1/2} - \left(1 + \frac{\sigma_n^2}{M_n^2} \right) \right\} M_n.$$

(ii) If now $\langle M_p^2 \rangle < \langle M_f^2 \rangle$, which occurs for high M_n, the mass distribution of packaged chains is necessarily truncated by the capsids, which can only accommodate the shortest chains. The mass distribution is modeled by a Schulz distribution [23] truncated at a cutoff mass $M_{\rm co}$. We

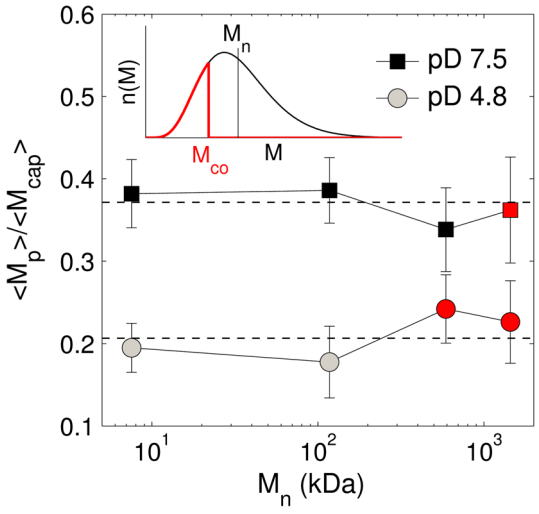

FIG. 3 (color online). Ratio of the mean mass of packaged dPSS $\langle M_p \rangle$ to the mean mass of capsid $\langle M_{\text{cap}} \rangle$ as a function of M_n at pD 7.5 (squares) and pD 4.8 (discs). The symbols in red indicate mass ratios computed with a truncated Schulz distribution. Dashed lines give the averages of the mass ratios in the least-squares sense: 0.37 for pD 7.5 and 0.21 for pD 4.8. The inset depicts the Schulz distribution $n(M)$ for free dPSS (black line) and its truncated version with a cutoff mass M_{co} (red line).

also assume that only one chain is packaged per VLP because the probability of packaging simultaneously several chains with a total mass below M_{co} becomes rapidly small as M_{co} diminishes [12]. The cutoff mass M_{co} can be computed from the truncated Schulz distribution $n(M)$ that returns the measured $\langle M_p^2 \rangle$, i.e.,

$$\langle M_p^2 \rangle = \int_0^{M_{\text{co}}} n(M) M^2 dM \left(\int_0^{M_{\text{co}}} n(M) dM \right)^{-1}$$

$$\text{with} \quad n(M) = \left(\frac{s}{M_n} \right)^s \frac{M^{s-1}}{\Gamma(s)} \exp\left(-s \frac{M}{M_n} \right),$$

where Γ denotes the gamma function and s a parameter verifying $s^{-1} \equiv (M_w/M_n) - 1$. The inset of Fig. 3 provides an example of a truncated Schulz distribution. Knowing M_{co}, M_n and s, the computation of $\langle M_p \rangle$ is straightforward.

The ratio $\langle M_p \rangle / \langle M_{\text{cap}} \rangle$ is plotted on Fig. 3 as a function of M_n. Remarkably, at fixed pD, $\langle M_p \rangle / \langle M_{\text{cap}} \rangle$ was invariant within the uncertainties for M_n spanning more than 2 orders of magnitude. In other words, capsids packaged an amount of dPSS proportional to their mass, either by uptaking a sufficient number of available chains, or by selectively retaining the shortest chains that could fit the capsid interior. It is worth mentioning here that, at given pD, $\langle M_{\text{cap}} \rangle$ was weakly varying (see Table II) because the number of capsomers in a capsid is subjected to energetic constraints reminiscent of the icosahedral symmetry [24]. By minimizing the free energy of packaged chains with respect to their number N_p, Zandi and van der Schoot found

TABLE II. Results from statistical model analysis.

d-PSS	$\langle M_{\text{cap}} \rangle$ (kDa)	$\langle M_p \rangle$ (kDa)	$\langle N_p \rangle$	$\langle Z_p \rangle / \langle Z_{\text{cap}} \rangle$[a]
		pD 7.5		
8k	1750 ± 66	670 ± 47	88 ± 6.2	-4.1 ± 0.45
120k	2580 ± 87	995 ± 69	8.5 ± 0.6	-4.1 ± 0.43
600k	2680 ± 140	905 ± 89	1.5 ± 0.15	-3.6 ± 0.55
1500k	2660 ± 140	960 ± 120	1[b]	-3.9 ± 0.70
		pD 4.8		
8k	1490 ± 67	290 ± 32	39 ± 4.2	-2.1 ± 0.32
120k	1750 ± 89	310 ± 60	2.7 ± 0.52	-1.9 ± 0.47
600k	1730 ± 75	419 ± 54	1[b]	-2.6 ± 0.45
1500k	1630 ± 55	370 ± 69	1[b]	-2.4 ± 0.54

[a]Ratio of the mean charge of packaged dPSS to the mean charge of the capsid interior.
[b]A truncated Schulz distribution was used. See text for details.

that the total number of packaged monomers $N_p N_n$ scales as R^2 rather than as the capsid volume, i.e., R^3 [2]. Since here $\langle M_p \rangle = \langle N_p \rangle N_n M_{\text{mono}}$, where M_{mono} is the molecular weight of a monomer, and because $\langle M_{\text{cap}} \rangle \propto R^2$, the Zandi–van der Schoot prediction can be reexpressed as $\langle M_p \rangle \propto (\gamma b / v) \langle M_{\text{cap}} \rangle$, where γ and b are effective chain-capsomer interaction strength and length, respectively, and v the excluded volume of Kuhn segments. The mass ratio turns out to be independent of M_n as found experimentally.

The effective interaction strength γ stems from the electrostatic interaction with the positive charges carried by the arginine-rich N-terminal arm of capsomers [21]. This flexible arm contains 10 cationic residues, all ionized in the actual range of pD. dPSS in turn carries nearly one negative charge per monomer due to its fully ionized sulfonate groups. Table II gives the ratio of charges carried by the packaged dPSS $\langle Z_p \rangle$ and by the basic residues that protrude into the capsid interior $\langle Z_{\text{cap}} \rangle$. Notice that $\langle Z_p \rangle / \langle Z_{\text{cap}} \rangle \propto \langle M_p \rangle / \langle M_{\text{cap}} \rangle$ and is thereby invariant for a given pD. The average charge ratio in the least-squares sense was estimated to be -4.0 at pD 7.5 and -2.3 at pD 4.8. Previously reported charge ratios were estimated to be -9.0 with 3.4-MDa PSS [7], and both -0.45 and -0.6 with 38-kDa PSS [9]. Our results are in better agreement with theory in the sense that the charge ratio is unchanged by the polyelectrolyte molecular weight. Our values also deviate from the ratio of ~ -1.6 found by Belyi and Muthumkumar with ssRNA [4]. They indicate a strong and unexpected overcharging of the capsid interior by the packaged dPSS. dPSS has a smaller intrinsic excluded volume v_0 than that of ssRNA. In a regime of strong electrostatic screening (the Debye length was $\sim$0.4 nm), $v \approx v_0$ [2], and we thereby expect from the Zandi–van der Schoot prediction an increasing mass (and charge) ratio as v_0 decreases. In fact, we did not even observe the packaging of viral RNA at pD 7.5, whereas dPSS could be readily packaged. It thus demonstrates that polyelectrolytes with a strongly hydrophobic backbone can be packaged more efficiently than viral RNA.

Lastly, the different values of $\langle M_p \rangle / \langle M_{\mathrm{cap}} \rangle$ at different pD emphasize the importance of the capsomer self-energy entering the total free energy. A higher pD increases the capsomer self-energy through the ionization of carboxylate groups which thus enhances the electrostatic repulsion between capsomers [25]. This causes the capsids to swell and to package a larger amount of polyelectrolyte in such a way that the mass ratio increases. The mechanism is reminiscent of the metal-free swelling transition that native virions exhibit at high pH [26]. The mean number of capsomers in VLPs $\langle N_{\mathrm{cap}} \rangle$ also varied with pD [12] and was not necessarily close to a multiple of 60 as required by the quasiequivalence principle [24]. VLPs were all larger than $T = 1$ capsids and smaller or similar in size to $T = 2$ capsids. Therefore, VLPs did not likely obey to the icosahedral symmetry but might rather exhibit local defects due to the presence of polyelectrolyte.

In summary, we have demonstrated that capsomers derived from a ssRNA plant virus can display a remarkably robust selectivity for packaging polyelectrolytes. This nonspecific selectivity takes the form of a balance between the mass of the capsid and that of the packaged polyelectrolytes, and is mainly, but not only, driven by electrostatic interactions. The present mechanism may be regarded as a primary way for a virus to package the required segments of its genome and it can explain in particular how CCMV distributes a similar amount of RNA in three particles. It must be mentioned, however, that specific signals embedded in the genome may favor the packaging. Also, a recent theoretical study suggested that the inherently branched RNA secondary structure could allow the viral RNA segments to out compete those coming from the infected host cells [27]. The kinetic pathways used to package polyelectrolytes might play a role as well and time-resolved investigations [28] could shed light on the nonequilibrium states visited by the system to achieve such a good efficacy in the self-assembly.

The authors thank A. L. N. Rao, Mauricio Comas-Garcia, William M. Gelbart, Stéphane Bressanelli, Didier Poncet, Françoise Lafuma, and Amélie Leforestier for their help. They also gratefully acknowledge the Forschungs-Neutronenquelle Heinz Maier-Leibnitz (Garching, Germany) and the Laboratoire Léon Brillouin (Saclay, France) for allocation of neutron beam time, as well as Marie-Sousai Appavou and Giulia Fadda for their assistance. The research was supported by the Triangle de la Physique (Contract No. 2009-073T), the European Commission, CNRS, UniverSud Paris, and the Polish Ministry of Science and Higher Education.

*guillaume.tresset@u-psud.fr
†Present address: Institut de Chimie et des Matériaux Paris-Est, Université Paris-Est, CNRS, 94320 Thiais, France.

[1] P. van der Schoot and R. Bruinsma, Phys. Rev. E **71**, 061928 (2005).
[2] R. Zandi and P. van der Schoot, Biophys. J. **96**, 9 (2009).
[3] A. Siber, A. L. Boi, and R. Podgornik, Phys. Chem. Chem. Phys. **14**, 3746 (2012).
[4] V. A. Belyi and M. Muthukumar, Proc. Natl. Acad. Sci. U.S.A. **103**, 17 174 (2006).
[5] S. I. Lee and T. T. Nguyen, Phys. Rev. Lett. **100**, 198102 (2008).
[6] F. D. Sikkema, M. Comellas-Aragons, R. G. Fokkink, B. J. M. Verduin, J. J. L. M. Cornelissen, and R. J. M. Nolte, Org. Biomol. Chem. **5**, 54 (2007).
[7] Y. Hu, R. Zandi, A. Anavitarte, C. M. Knobler, and W. M. Gelbart, Biophys. J. **94**, 1428 (2008).
[8] V. Mengarelli, L. Auvray, D. Pastré, and M. Zeghal, Eur. Phys. J. E **34**, 127 (2011).
[9] R. D. Cadena-Nava, Y. Hu, R. F. Garmann, B. Ng, A. N. Zelikin, C. M. Knobler, and W. M. Gelbart, J. Phys. Chem. B **115**, 2386 (2011).
[10] Y. Ren, S.-M. Wong, and L.-Y. Lim, J. Gen. Virol. **87**, 2749 (2006).
[11] *Viruses and Nanotechnology*, edited by M. Manchester and N. F. Steinmetz (Springer, New York, 2009).
[12] See Supplemental Material at http://link.aps.org/supplemental/10.1103/PhysRevLett.113.128305, which includes Refs. [13–20], for sample preparation, fitting models, and analysis parameters.
[13] A. Ali and M. J. Roossinck, J. Virol. Methods **141**, 84 (2007).
[14] H. Vink, Macromolecular Chemistry **182**, 279 (1981).
[15] A. K. Covington, M. Paabo, R. A. Robinson, and R. G. Bates, Anal. Chem. **40**, 700 (1968).
[16] R. P. May and V. Nowotny, J. Appl. Crystallogr. **22**, 231 (1989).
[17] T. R. Shaikh, H. Gao, W. T. Baxter, F. J. Asturias, N. Boisset, A. Leith, and J. Frank, Nat. Protoc. **3**, 1941 (2008).
[18] B. Jacrot, C. Chauvin, and J. Witz, Nature (London) **266**, 417 (1977).
[19] T. Hattori, R. Hallberg, and P. L. Dubin, Langmuir **16**, 9738 (2000).
[20] J. Gummel, F. Cousin, and F. Boué, Macromolecules **41**, 2898 (2008).
[21] R. D. Cadena-Nava, M. Comas-Garcia, R. F. Garmann, A. L. N. Rao, C. M. Knobler, and W. M. Gelbart, J. Virol. **86**, 3318 (2012).
[22] M. Castelnovo, D. Muriaux, and C. Faivre-Moskalenko, New J. Phys. **15**, 035028 (2013).
[23] M. Rubinstein and R. H. Colby, *Polymer Physics* (Oxford University Press, Oxford, 2003).
[24] R. F. Bruinsma, W. M. Gelbart, D. Reguera, J. Rudnick, and R. Zandi, Phys. Rev. Lett. **90**, 248101 (2003).
[25] J. R. Vega-Acosta, R. D. Cadena-Nava, W. M. Gelbart, C. M. Knobler, and J. Ruiz-Garca, J. Phys. Chem. B **118**, 1984 (2014).
[26] J. A. Speir, S. Munshi, G. Wang, T. S. Baker, and J. E. Johnson, Structure **3**, 63 (1995).
[27] G. Erdemci-Tandogan, J. Wagner, P. van der Schoot, R. Podgornik, and R. Zandi, Phys. Rev. E **89**, 032707 (2014).
[28] G. Tresset, C. Le Cœur, J.-F. Bryche, M. Tatou, M. Zeghal, A. Charpilienne, D. Poncet, D. Constantin, and S. Bressanelli, J. Am. Chem. Soc. **135**, 15 373 (2013).